Smectic Vortex Phase in Optimally Doped $YBa_2Cu_3O_7$ Thin Films

S. A. Baily,[1,2,*] B. Maiorov,[1,2] H. Zhou,[1] F. F. Balakirev,[2] M. Jaime,[2] S. R. Foltyn,[1] and L. Civale[1]

[1]*Superconductivity Technology Center, Los Alamos National Laboratory, Los Alamos, New Mexico, 87545, USA*

[2]*National High Magnetic Field Laboratory, Los Alamos National Laboratory, Los Alamos, New Mexico, 87545, USA*

(Received 10 October 2007; published 18 January 2008)

Angular dependent resistivity measurements of optimally doped $YBa_2Cu_3O_7$ films in fields H pulsed to 50 T are presented. Up to the highest H, the vortex melting field H_m increases and vortex motion is reduced for $\mathbf{H}$ aligned with the correlated pinning centers along the main crystalline axes, otherwise 3D anisotropic scaling describes the vortex dynamics. For $\mathbf{H} \parallel ab$, the rapid increase in H_m at low temperatures and a critical exponent analysis near H_m confirm the presence of the liquid-crystalline smectic phase predicted for layered superconductors.

DOI: 10.1103/PhysRevLett.100.027004 PACS numbers: 74.25.Qt, 61.30.Eb, 64.70.M−, 74.78.Bz

A number of predictions for exotic vortex behavior in the high-density or high-field limit remain largely unconfirmed [1–9], because only a few experimental studies have focused on superconducting vortex phases in fields above 20 T [10–12]. One new feature found in high temperature superconductors is the appearance of a thermodynamic phase transition from a solid to a liquid vortex phase as the temperature or the magnetic field is raised [13]. The nature of both the solid and the liquid are affected by the presence of different types of pinning centers [2,14–16]. This has been studied in high temperature superconductors with naturally grown and artificially induced defects [17–22]. Angular dependent measurements have played a key role in distinguishing the anisotropic properties and nature of these different transitions [17–20].

For 3D anisotropic superconductors in the presence of pointlike defects the angular dependence of the vortex liquid-solid transition is governed by the electronic-mass anisotropy (γ) [16], and scales with $\varepsilon(\theta)H = H[\cos^2(\theta) + \gamma^{-2}\sin^2(\theta)]^{-1/2}$, where θ is the angle between the applied magnetic field ($\mathbf{H}$) and the crystallographic c axis. Pinning by correlated defects leads to a solid phase known as Bose glass and can be distinguished from random pointlike defects by the presence of a peak in the angular dependence of the melting line when H is aligned with the defects [14,15,18–20].

When $\mathbf{H}$ is applied along the crystallographic a-b plane, the vortex matter in high T_c superconductors is expected to be particularly rich since random and columnar pinning centers coexist with equally spaced planar pinning centers. The latter are created by the layered crystal structure, which gives rise to *intrinsic pinning* [2,3,23]. In $YBa_2Cu_3O_7$ (YBCO), the field at which the separation between vortices is equal to the distance between layers is ≈ 230 T, similar to H_{c2} at $T = 0$. One cannot hope to space pinning centers in YBCO more closely than the distance between copper-oxygen planes. First Kwok *et al.* [17,24], then Grigera *et al.* [25], explored the nature of the vortex solid-liquid transition for $\mathbf{H} \parallel ab$ at low fields ($H < 8$ T) and high temperatures in optimally doped YBCO single crystals. However, Gordeev *et al.* [26] used underdoped single crystals to show that it was possible to observe a key signature of intrinsic pinning (the appearance of a smectic phase), i.e., an upward turn of the melting field (H_m), with an almost temperature independent H_m line [2,3,26]. Gordeev *et al.* also predicted that in order to observe this phenomena in optimally doped YBCO ($\gamma =$ 5–7) $H \sim 50$ T would be required, a field not yet attainable by DC magnets. There are several related descriptions for this rapid increase in H_m [2–9], which indicate that this transition is favorable in strongly layered materials (with higher electronic-mass anisotropy, $\gamma > 10$). The smectic phase is also predicted to be robust in the presence of other types of strong pinning [9]. Repeated attempts have been made to measure this effect in materials with low anisotropy [24–27]. By performing angular dependent resistivity measurements in a pulsed field (up to 50 T), we are finally able to observe this effect in optimally doped YBCO ($\gamma =$ 6). Moreover, by studying thin films with high critical current density (J_c) we also explore how strong pinning affects the liquid near the vortex solid-liquid transition. This also improves the signal to noise ratio and allows us to extract the critical exponent s at the onset of the transition.

In this Letter, we present the first evidence for a smectic phase in optimally doped, high-J_c YBCO films just below 80 K in fields near 50 T, in accordance with Gordeev's prediction [26]. By studying intrinsic pinning in a film with high J_c we address the nature of the transition, its effect on the liquid state, and its comparison with results obtained for $\mathbf{H} \parallel c$ where correlated defects are randomly distributed. We also find that anisotropic scaling holds to 50 T, except along the crystalline axes, and we interpret this as an indication that the vortices remain three dimensional throughout the entire field range. Angular dependent measurements enable us to show that along the main crystallographic axes melting-field enhancement due to correlated pinning remains dominant up to 50 T.

We grew 0.2 μm of YBCO on $SrTiO_3$ by pulsed laser deposition under the carefully controlled and highly optimized conditions needed to produce state-of-the-art J_c

[28]. This film has an x-ray rocking curve with a full width at half maximum of $<0.5°$ for the (005) peak, critical temperature $T_c = 90.2$ K, and $J_c = 4.8$ MA/cm^2 at 75.5 K in self-field. Obtaining this J_c requires many dislocations and other defects that pin vortices and few current-blocking defects (voids, a-axis grains, and high angle grain boundaries), as described in detail in Ref. [28]. The film was photolithographically patterned and acid etched to form a 3-mm-long, 250-μm-wide bridge. Evaporated silver electrical-contact pads were added and annealed in oxygen. In our study, a low 52 A/cm^2 ac current density (100 KHz) is applied along the bridge which is oriented on a rotating platform such that the current is always perpendicular to $\mathbf{H}$. A 50-ms magnetic field pulse is applied while monitoring the resistivity with a lock-in amplifier. No evidence of self-heating was observed.

Figure 1 shows the resistivity vs scaled magnetic field oriented at different angles for $T = 80$ and 85 K. The upper x-axis $[\varepsilon(\theta)H]$ and the lower x-axis $[\gamma\varepsilon(\theta)H]$ reflect the scaled fields with respect to $\mathbf{H} \parallel c$ and $\mathbf{H} \parallel ab$, respectively. At intermediate angles an electronic-mass anisotropy of $\gamma = 6 \pm 0.2$ can scale the entire curve at all temperatures examined. This value is consistent with the slight overdoping obtained by the oxygen annealing. Near the crystalline axes, H_m increases due to correlated pinning (Figs. 1 and 2). For $\mathbf{H} \parallel c$, the dissipation in the vortex-liquid state remains smaller than the scaled curves up to twice the H_m, and the resistivity does not converge with the scaled curves until 40% of ρ_N (the resistivity at 100 K). With $\mathbf{H} \parallel ab$ planes, the dissipation is further reduced, remaining smaller than the scaled curves up to the highest field achieved; at 85 K, the dissipation reduction is still significant at 3 times H_m with $\rho = 0.4\rho_N$. This shows that intrinsic pinning not only increases the onset of dissipation but arrests the motion of vortices in the vortex-liquid state. At 80 K, the c-axis correlated defects and the intrinsic pinning increase $\varepsilon(\theta)H_m$ to similar values. However, the slower resistivity rise for intrinsic pinning indicates that the layered structure is much better at "pinning" the vortex liquid than the pinning centers aligned with the c axis or at intermediate angles. This is probably related to the extremely high density of intrinsic pinning centers and vortex motion by the sliding of double kinks.

Figure 2 displays the angular dependence of H_m for some selected temperatures, determined by resistivity criteria. At intermediate angles H_m follows $\varepsilon(\theta)$ but deviates when close to $\theta = 0°$ and 90°. As the temperature is lowered the height of the c-axis peak increases [see Fig. 2(a)] while its width remains constant in contrast to the peak at the ab which becomes sharper. This sharp peak [Fig. 2(b)] was used to align the sample and verify reproducibility of rotational position.

Figure 3 shows the temperature dependence of the melting field at 45°, 65°, 0°, and 90° with the melting field scaled by electronic-mass anisotropy. As expected from the curves shown in Figs. 1 and 2, away from the main crystalline axes the data scale with anisotropy (using $\gamma = 6$). The temperature dependence of the scaled points can be fit by $H_m = C(T_c - T)^a$ with $a = 1.4$. This scaling as a function of angle and temperature indicates that random pointlike pinning is dominant, and the solid-liquid vortex transition remains of the same type up to the highest field achieved (50 T). On the other hand, along the main crystallographic directions, correlated pinning increases H_m. Still, the temperature dependence of H_m is similar both for the random part $(50 < |\theta| < 85)$ and for $\mathbf{H} \parallel c$ with $a = 1.4$. This holds true up to the highest field and lowest temperature measured ($T = 45$ K and $H = 50$ T), half of T_c. Only the coefficient of proportionality, C, changes between intermediate angles and $\mathbf{H} \parallel c$, as shown by the fits to the data in Fig. 3. This also indicates that even though the c-axis correlated defects have been far outnumbered at

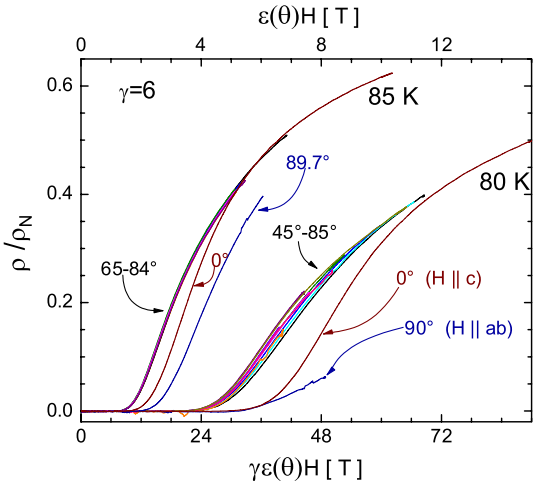

FIG. 1 (color online). Normalized resistivity vs magnetic field scaled with angle using anisotropic scaling at 80 and 85 K. Minor ($< 2\%$) systematic corrections to the scaled magnetic field have been applied to account for variations in the sample temperature of <0.1 K.

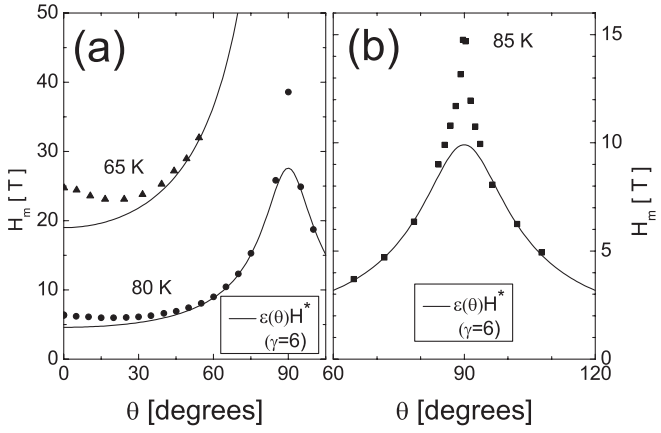

FIG. 2. The melting field vs angle at 65 and 80 K (a), and at 85 K (b). (a) and (b) use criteria of 2% and 1% of ρ_N, respectively. The lines are proportional to the anisotropic scaling function $\epsilon(\theta)H$ using $\gamma = 6$.

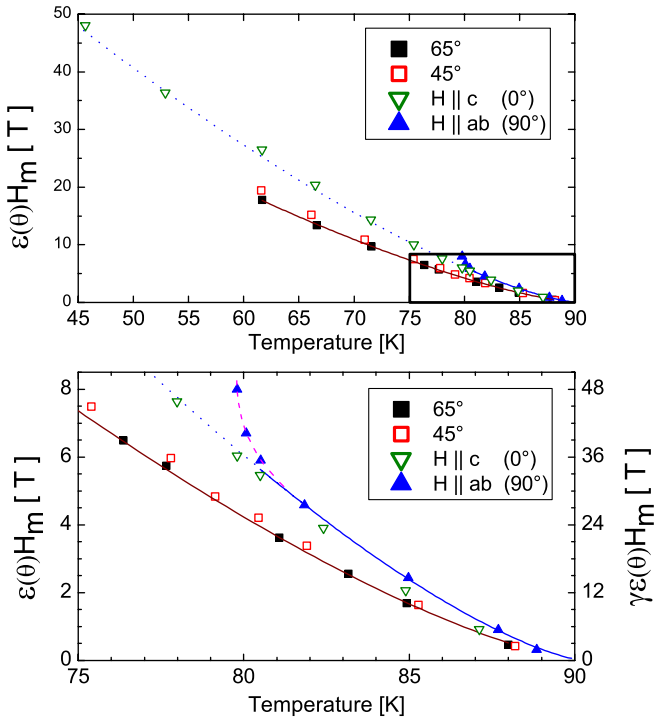

FIG. 3 (color online). Temperature dependence of the melting line at various angles. Solid lines: fits to the data using $H_m = C(T_c - T)^{1.4}$ at 65° and $\mathbf{H} \parallel ab$. Dotted line: extension of the fit for $\mathbf{H} \parallel ab$. Dashed line: guide to the eye.

these fields, their stabilizing (or entropy reducing) effect still persists, a similar feature to that observed in twinned single crystals [20]. The similar temperature dependence for $\varepsilon(\theta)H_m$ at intermediate angles and at the c axis suggests that the mechanisms or origins of the melting are similar. The mechanism is probably closely related to the interstitial liquid proposed by Radzihovsky [1].

For $\mathbf{H} \parallel ab$, at high temperatures, H_m behaves similarly as a function of temperature to that of $\mathbf{H} \parallel c$, in terms of both the exponent $a = 1.4$ and the proportionality constant C, as can be observed in Fig. 3. This holds true down to 80 K, which corresponds to $H \sim 40$ T and to a scaled (to the c axis) field near 7 T. Below 80 K, H_m increases much more rapidly and $\rho(H)$ shows a much slower increase with H than at 85 K (Fig. 1). The rapid rise of H_m (Fig. 3) could be an indication that the vortex cores are becoming small enough to be localized between the Cu-O planes, and it is reminiscent of the results for underdoped YBCO single crystals measured in DC fields [26]. The fact that this is observed in a low-anisotropy, high-J_c thin film, is remarkable and corroborates the robustness predicted for this vortex phase by Balents and Nelson [29]. Although our results are in agreement with Gordeev *et al.*'s expectations [26], Lundqvist *et al.* report a similar effect with current applied along the c axis [27], which is not expected for a smectic phase.

To further elucidate the nature of this resistive transition we turn to the critical behavior. If this is the vortex phase predicted by Balents and Nelson, then the critical exponents below the multicritical point are expected to be similar to those of a nematic to smectic-A transition, rather than those of transitions to a Bose glass or vortex glass [29]. From the resistivity vs field data we are able to extract the critical exponent s using $\rho \propto (H - H_m)^s$. In practice, this is a delicate task since changes in H_m will affect the value of s; therefore obtaining those parameters independently is highly desirable. We have used a windowing procedure similar to that used by Sebastian *et al.* [30] to extract critical exponents independently of H_m. A small background signal (not observable in Fig. 1) was subtracted from all curves. We obtain the same critical exponents at $\theta = 65°$ ($s = 2.5 \pm 0.3$), 45° (3.2 ± 0.5), and 0° (3.1 ± 0.6) (see Fig. 4). The data taken at $\theta = 90°$ ($\mathbf{H} \parallel ab$) above 82 K also have the same critical exponent. Our value ($s = 3.0 \pm 0.5$) is in good agreement with measured critical exponents reported for the Bose-glass transition in twinned crystals (2.8 ± 0.2 [19] or 2.7 ± 0.3 [20]). Even though we obtain excellent scaling with anisotropy at intermediate angles, s is much smaller than the $s = 5.3 \pm 0.7$ [31] obtained in proton irradiated single crystals. This may be surprising, but one must bear in mind that our film has columnar defects along both crystalline axes. For $T < 81$ K, when the melting field begins to rise more rapidly, the critical exponent decreases to values as low as $s = 0.6$, significantly smaller than the value expected and measured for Bose- or vortex-glass states. For a nematic to smectic-A transition $s = 1 - \alpha = 3\nu - 1$ [2,32]. Measured values for the nematic-smectic-A correlation-length exponent ν in liquid crystals range from 0.37 to 0.83 [33], implying $0.1 < s < 1.5$, in accordance with the values of s that we find. The fact that s is similar at higher temperatures for $\mathbf{H} \parallel ab$ and at all temperatures for other angles suggests a common origin of the melting

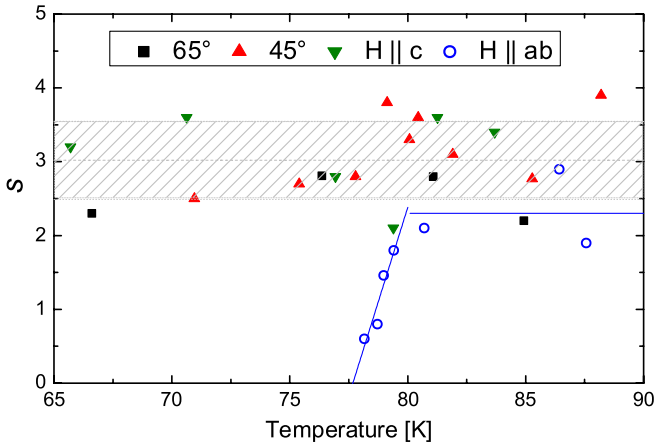

FIG. 4 (color online). Critical exponent s vs T at various angles. The shaded area is within one σ of the average value for $\mathbf{H} \parallel c$, $\theta = 45°$, and $\theta = 65°$. Solid lines: linear fit to the coldest four data points and the average of the warmest three for $\mathbf{H} \parallel ab$.

transition, especially when taken together with the exponent $a = 1.4$ in the H-T diagram mentioned previously.

This change in the dynamic response of the vortex liquid near the liquid-solid transition is also observed in the vortex solid through J_c measurements, where the nonlinear nature of the response upon exceeding the critical current changes abruptly for $T < 80$ K and $\mathbf{H} \parallel ab$ [34]. At these temperatures, the nonlinear current-voltage curves can be well described as a power law with $V \propto (I/I_c)^n$. Generally a direct relation is found between n and I_c since n is (to first order) proportional to the pinning energy. However, for $T < 80$ K an inverse relation between I_c and n is observed when $\mathbf{H}$ reaches the ab plane, with the V-I curves becoming flatter (smaller n) as I_c increases, an indication of *intrinsic pinning* [34]. This is caused by double kinks (the depinning mechanism of *intrinsic pinning*) which slide at no energy cost upon application of a transport current. As the portion of the vortex that moves is much smaller in the intrinsic pinning situation, the dissipation is reduced in comparison to that of expanding vortex rings that occur in the depinning of other defects. This might also be the case for the reduced dissipation in the liquid at high field for $\mathbf{H} \parallel ab$ observed in Fig. 1.

The changes in the solid and in the solid-liquid transition are indicative of intrinsic pinning becoming relevant for $T < 80$ K. These data provide convincing evidence for an intrinsic pinning mechanism both in the solid and at the liquid-solid transition in high-J_c, low-anisotropy YBCO films. The low critical exponents we obtain for $T < 80$ K and $\mathbf{H} \parallel ab$ are consistent with a smectic phase.

In summary, the vortices remain 3D in fields up to 50 T and temperatures down to 45 K (half of T_c), and an enhancement in H_m coming from correlated pinning is observed when the field is applied along $\mathbf{H} \parallel c$ and $\mathbf{H} \parallel ab$. Well into the liquid when defect-induced correlated pinning becomes ineffective, anisotropic scaling holds even when $\mathbf{H}$ is applied along the direction of correlated defects. Intrinsic pinning still remains effective at these fields and not only greatly increases H_m, but affects the liquid state at much higher dissipation levels than the ''strong pinning'' induced by defects along the c axis. Once vortex cores become small enough to be localized between the copper-oxygen planes, intrinsic pinning becomes even more effective at increasing H_m and reducing dissipation in the liquid (with an approximately linear increase in dissipation with H). This effect is not the result of a change in nature of vortices at high fields, as it does not occur with fields up to 50 T applied in other directions (several times higher in scaled field). We present the first evidence that this behavior is robust against the presence of strong pinning and is still present in a material with low anisotropy, where vortices are 3D in nature at other orientations. The critical exponents obtained indicate that intrinsic pinning leads to a different vortex-solid phase at low temperatures and are consistent with the conclusion that this phase is indeed a smectic phase.

This work is supported by an NHMFL IHRP grant, by U.S. NSF, by U.S. DOE, and by the state of Florida. We thank V. S. Zapf for helpful discussions regarding critical exponents.

*sbaily@lanl.gov

[1] L. Radzihovsky, Phys. Rev. Lett. **74**, 4923 (1995).
[2] L. Balents and D. R. Nelson, Phys. Rev. Lett. **73**, 2618 (1994).
[3] X. Hu and M. Tachiki, Phys. Rev. B **70**, 064506 (2004).
[4] K. B. Efetov, Sov. Phys. JETP **49**, 905 (1979).
[5] L. Bulaevskii and J. R. Clem, Phys. Rev. B **44**, 10 234 (1991).
[6] L. V. Mikheev and E. B. Kolomeisky, Phys. Rev. B **43**, 10 431 (1991).
[7] B. Horovitz, Phys. Rev. Lett. **67**, 378 (1991).
[8] S. E. Korshunov and A. I. Larkin, Phys. Rev. B **46**, 6395 (1992).
[9] L. Balents, M. C. Marchetti, and L. Radzihovsky, Phys. Rev. B **57**, 7705 (1998).
[10] Y. Skourski *et al.*, Physica (Amsterdam) **346B–347B**, 325 (2004).
[11] N. Miura *et al.*, Physica (Amsterdam) **319B**, 310 (2002).
[12] J. Hänisch *et al.*, Supercond. Sci. Technol. **20**, 228 (2007).
[13] E. Brézin, D. R. Nelson, and A. Thiaville, Phys. Rev. B **31**, 7124 (1985).
[14] M. P. A. Fisher, Phys. Rev. Lett. **62**, 1415 (1989).
[15] D. R. Nelson and V. M. Vinokur, Phys. Rev. B **48**, 13 060 (1993).
[16] G. Blatter *et al.*, Rev. Mod. Phys. **66**, 1125 (1994).
[17] W. K. Kwok *et al.*, Phys. Rev. Lett. **72**, 1088 (1994).
[18] L. Civale *et al.*, Phys. Rev. Lett. **67**, 648 (1991).
[19] S. A. Grigera *et al.*, Phys. Rev. Lett. **81**, 2348 (1998).
[20] B. Maiorov and E. Osquiguil, Phys. Rev. B **64**, 052511 (2001).
[21] J. R. Thompson *et al.*, Physica (Amsterdam) **200A**, 395 (1993).
[22] L. Civale *et al.*, Appl. Phys. Lett. **84**, 2121 (2004).
[23] M. Tachiki and S. Takahashi, Solid State Commun. **70**, 291 (1989).
[24] W. K. Kwok *et al.*, Phys. Rev. Lett. **67**, 390 (1991).
[25] S. A. Grigera *et al.*, Phys. Rev. B **59**, 11 201 (1999).
[26] S. N. Gordeev *et al.*, Phys. Rev. Lett. **85**, 4594 (2000).
[27] B. Lundqvist *et al.*, Phys. Rev. B **64**, 060503(R) (2001).
[28] S. R. Foltyn *et al.*, Nat. Mater. **6**, 631 (2007).
[29] L. Balents and D. R. Nelson, Phys. Rev. B **52**, 12 951 (1995).
[30] S. E. Sebastian *et al.*, Phys. Rev. B **72**, 100404(R) (2005).
[31] A. M. Petrean *et al.*, Phys. Rev. Lett. **84**, 5852 (2000).
[32] D. Djurek, J. Baturić-Rubčić, and K. Franulovi, Phys. Rev. Lett. **33**, 1126 (1974).
[33] B. S. Andereck, Int. J. Mod. Phys. B **9**, 2139 (1995).
[34] L. Civale *et al.*, IEEE Trans. Appl. Supercond. **15**, 2808 (2005).